

This discussion paper is/has been under review for the journal Atmospheric Chemistry and Physics (ACP). Please refer to the corresponding final paper in ACP if available.

Time-resolved characterization of primary and secondary particle emissions of a modern gasoline passenger car

P. Karjalainen¹, H. Timonen², E. Saukko¹, H. Kuuluvainen¹, S. Saarikoski²,
P. Aakko-Saksa³, T. Murtonen³, M. Dal Maso¹, E. Ahlberg^{4,5}, B. Svenningsson⁵,
W. H. Brune⁶, R. Hillamo², J. Keskinen¹, and T. Rönkkö¹

¹Aerosol Physics Laboratory, Department of Physics, Tampere University of Technology, P.O. Box 692, 33101 Tampere, Finland

²Atmospheric Composition Research, Finnish Meteorological Institute, P.O. Box 503, 00101 Helsinki, Finland

³VTT Technical Research Centre of Finland Ltd., P.O. Box 1000, 02044 VTT, Espoo, Finland

⁴Centre for Environmental and Climate research, Lund University, Box 118, 22100 Lund, Sweden

⁵Division of Nuclear Physics, Lund University, Box 118, 221 00 Lund, Sweden

⁶Department of Meteorology, Pennsylvania State University, University Park, PA, USA

Time-resolved
primary and
secondary particle
emissions of a
gasoline vehicle

P. Karjalainen et al.

Title Page

Abstract

Introduction

Conclusions

References

Tables

Figures

◀

▶

◀

▶

Back

Close

Full Screen / Esc

Printer-friendly Version

Interactive Discussion

Received: 10 November 2015 – Accepted: 16 November 2015
– Published: 25 November 2015

Correspondence to: T. Rönkkö (topi.ronkko@tut.fi)

Published by Copernicus Publications on behalf of the European Geosciences Union.

ACPD

15, 33253–33282, 2015

**Time-resolved
primary and
secondary particle
emissions of a
gasoline vehicle**

P. Karjalainen et al.

Title Page

Abstract

Introduction

Conclusions

References

Tables

Figures



Back

Close

Full Screen / Esc

Printer-friendly Version

Interactive Discussion



Abstract

Changes in traffic systems and vehicle emission reduction technologies significantly affect traffic-related emissions in urban areas. In many densely populated areas the amount of traffic is increasing, keeping the emission level high or even increasing. To understand the health effects of traffic related emissions, both primary and secondary particles that are formed in the atmosphere from gaseous exhaust emissions need to be characterized. In this study we used a comprehensive set of measurements to characterize both primary and secondary particulate emissions of a modern gasoline passenger car. Our aerosol particle study covers the whole process chain in emission formation, from the engine to the atmosphere, and takes into account also differences in driving patterns. We observed that in mass terms, the amount of secondary particles was 13 times higher than the amount of primary particles. The formation, composition, number, and mass of secondary particles was significantly affected by driving patterns and engine conditions. The highest gaseous and particulate emissions were observed at the beginning of the test cycle when the performance of the engine and the catalyst was below optimal. The key parameter for secondary particle formation was the amount of gaseous hydrocarbons in primary emissions; however, also the primary particle population had an influence. Thus, in order to enhance human health and wellbeing in urban areas, our study strongly indicates that in future legislation, special attention should be directed into the reduction of gaseous hydrocarbons.

1 Introduction

Vehicular emissions deteriorate the air quality locally (Wehner et al., 2002; Pirjola et al., 2012; Lähde et al., 2014) and contribute significantly to the air pollution levels in urban areas. Air pollution components like particulate matter contribute to adverse health effects of people (e.g. Pope III and Dockery, 2006). The human exposure on pollutants in urban environments is the highest in the vicinity of traffic. In order to reduce the ad-

Time-resolved primary and secondary particle emissions of a gasoline vehicle

P. Karjalainen et al.

Title Page

Abstract

Introduction

Conclusions

References

Tables

Figures



Back

Close

Full Screen / Esc

Printer-friendly Version

Interactive Discussion



Time-resolved primary and secondary particle emissions of a gasoline vehicle

P. Karjalainen et al.

Title Page

Abstract

Introduction

Conclusions

References

Tables

Figures

◀

▶

◀

▶

Back

Close

Full Screen / Esc

Printer-friendly Version

Interactive Discussion

verse health effects and exposure of people by pollutants, the emission regulation for motor vehicles include limits for particulate mass (PM), and in Europe for some vehicle types, particle number (PN), of which the PN limit is considered to be stricter. Limits for gaseous compounds cover total hydrocarbon emissions, nitrogen oxides and carbon monoxide. Both particulate and gaseous emissions are strongly affected by technology development (e.g. catalysts and filters), driven by legislation activities. This technology development has, in general also other effects than required by emission legislation, for example fuel sulfur content limitations affect the emissions of nanoparticles. It should be noted that semi-volatile compounds (e.g. low-volatility organics, sulphuric compounds) are not directly regulated even though they are partially detected in the gravimetric PM determination as particles or adsorbed gas phase artefacts (Chase et al., 2004; Högström et al., 2012).

In the gasoline vehicle fleet the port-fuel injection (PFI) techniques has been widely replaced by gasoline direct injection (GDI) technologies due to the need to decrease fuel consumption and NO_x emissions of passenger cars (e.g. Alkidas, 2007; CARB, 2010). The disadvantage of GDI technologies is the increased primary particle emission (Aakko and Nylund, 2003; Mohr et al., 2006; Braisher et al., 2010). The GDI vehicle exhaust particle number concentrations are typically significantly lower than the diesel exhaust particle concentrations without a diesel particulate filter (DPF) but higher than concentrations with a DPF (Mathis et al., 2005). The GDI engine exhaust particle size distribution has been observed to be bi-modal (Barone et al., 2012; Sementa et al., 2012; Sgro et al., 2012; Maricq et al., 1999; Karjalainen et al., 2014; Pirjola et al., 2015a) and the emission is dominated by elemental carbon (EC) (Maricq et al., 2012). Organic carbon (OC) constitutes only a small fraction of particle emissions. Particles are (in number) mainly in ultrafine particle sizes (e.g. Maricq et al., 1999; Harris and Maricq, 2001; Khalek et al., 2010; Karjalainen et al., 2014). According to the study of Karjalainen et al. (2014), the GDI exhaust particles can be divided into four different types: spherical amorphous particles consisting of carbon with mean particle size between 10 and 20 nm (see also Sgro et al., 2012; Barone et al., 2012), agglomer-

Time-resolved primary and secondary particle emissions of a gasoline vehicle

P. Karjalainen et al.

Title Page

Abstract

Introduction

Conclusions

References

Tables

Figures

◀

▶

◀

▶

Back

Close

Full Screen / Esc

Printer-friendly Version

Interactive Discussion



ated soot like particles with mean particle size between 30 and 60 nm, lubricant oil originating particles consisting of metallic ash components (Rönkkö et al., 2014) and semivolatile nucleation particles (see also Mathis et al., 2005; Li et al., 2013). The highest emissions of primary particles take place under acceleration and deceleration conditions (Karjalainen et al., 2014).

Secondary aerosol formation happens in the atmosphere through oxidation processes that tend to lower the saturation vapor pressures of organic species. Thus, more oxidized compounds, mostly organic compounds, are more likely found in the particle phase (Robinson et al., 2007). Fresh exhaust emissions contain a variety of different organic compounds, in the scale of hundreds or thousands of different components (Rogge et al., 1993). Part of those has low saturation vapor pressure already when emitted and thus they are observed in primary particulate emission or in particulate phase after the exhaust has been diluted rapidly into the atmospheric conditions (Tobias et al., 2001; Sakurai et al., 2003; Arnold et al., 2012; Pirjola et al., 2015b). However, even the majority of organic compounds in the exhaust are primarily emitted to atmosphere in gaseous phase. Also, sulfur compounds such as SO₂ as well as nitrogen oxides can play a role in the secondary aerosol formation processes in the atmosphere.

There are studies of engine exhaust related secondary organic aerosol (SOA) formation for gasoline (Suarez-Bertoa et al., 2015; Nordin et al., 2013) and diesel vehicles (e.g. Weitkamp et al., 2007; Chirico et al., 2010; Gordon et al., 2013). In these, the secondary particulate emissions of gasoline vehicles have been studied using a smog chamber so that diluted exhaust gas has been led to the smog chamber during a test cycle, a constant speed operation or idling condition (Suarez-Bertoa et al., 2015; Nordin et al., 2013). However, in the emission's perspective this represents only the average over the test, and more detailed analysis of the effect of driving pattern and engine conditions on SOA formation is lacking. With the potential aerosol mass (PAM) concept (Kang et al., 2007) SOA emissions can be studied in a shorter time scale (minutes). The PAM is a flow-through type reactor that uses UV lamps to form oxidants (O₃,

Time-resolved primary and secondary particle emissions of a gasoline vehicle

P. Karjalainen et al.

Title Page

Abstract

Introduction

Conclusions

References

Tables

Figures

◀

▶

◀

▶

Back

Close

Full Screen / Esc

Printer-friendly Version

Interactive Discussion

commercial E10 (max 10 % ethanol). The driving cycle used in the study was New European Driving Cycle (NEDC). The European exhaust emissions driving cycle “NEDC” is defined in the UN ECE R83 regulation. The car was tested on a chassis dynamometer in a climatic test cell at +23 °C. NEDC totals 11.0 km, divided into three test phases to study emissions at cold start and with warmed-up engines. The first and second test phases (later called as cold start urban driving cycle, CSUDC, and hot urban driving cycle, HUDC) each consisted of 2.026 km driving, and the third test phase, the extra-urban driving cycle (EUDC), was 6.955 km.

Particle sampling was conveyed by a partial exhaust sampling system (Ntziachristos et al., 2004) at the exhaust transfer line. The sampling system consisted of a porous tube diluter (PTD) (dilution ratio (DR) 12), residence time chamber (2.5 s) and secondary dilution conducted by Dekati Diluter (DR 8). In terms of exhaust nucleation particle formation, the sampling system mimics the real exhaust dilution and nanoparticle formation processes in the atmosphere (Rönkkö et al., 2006; Keskinen and Rönkkö, 2010). A PAM (Potential aerosol mass) chamber (Lambe et al., 2011) was used to evaluate SOA formation during the NEDC cycle. The PAM chamber was installed between the ageing chamber and secondary dilution units of sampling system. The sample flow through the PAM chamber was set to $\sim 9.75 \text{ L min}^{-1}$ resulting average residence time of 84 s. The voltage of the two UV lamps was at maximum value, 190 V. Relative humidity (RH) and temperature were measured prior to the PAM with the typical values of 60 % and 22 °C, respectively. Ozone concentration after the PAM was on average 6 ppm. The PAM chamber was calibrated using average experiment conditions and following the same procedure described by Lambe et al. (2011). All cycles were firstly run without the PAM chamber to measure primary emissions and secondly with the PAM chamber in order to study the formation of secondary particulate material.

The particle instrumentation was located downstream of the secondary diluter. The particle size distributions were measured on-line (1 Hz time resolution) with a High-resolution low-pressure impactor (HRLPI) (Arffman et al., 2014), fitted into an ELPI bodywork to replace the original charger and impactor, and an Engine exhaust parti-

Time-resolved primary and secondary particle emissions of a gasoline vehicle

P. Karjalainen et al.

Title Page

Abstract

Introduction

Conclusions

References

Tables

Figures

◀

▶

◀

▶

Back

Close

Full Screen / Esc

Printer-friendly Version

Interactive Discussion

cle sizer (EEPS, TSI Inc.) (Johnson et al., 2004). The particle number concentration was also measured with an ultrafine condensation particle counter (UCPC, TSI Inc. model 3025) that was located downstream of a passive nanoparticle diluter (DR 42). A SP-AMS was used to measure chemical composition (ions, organic carbon, refractory black carbon and some metals) of emitted submicron (50–800 nm) particulate matter (PM). SP-AMS is a high resolution time-of-flight aerosol mass spectrometer (HR-ToF-AMS) with added laser (intracavity Nd:YAG, 1064 nm) vaporizer (Schwarz et al., 2008). The HR-ToF-AMS is described in detail by (DeCarlo et al., 2006; Jayne et al., 2000) and SP-AMS is described by (Schwarz et al., 2008). Briefly, in the SP-AMS an aerodynamic lens is used to form a narrow beam of particles that is transmitted into the detection chamber, where the species are flash-vaporized with the laser and non-BC containing particles are vaporized either by normal tungsten vaporizer in (600) to analyze inorganic ion and OC concentrations and with SP laser (intracavity Nd:YAG, 1064 nm) in order to analyze black carbon and metals. The vaporized compounds are ionized using electron impact ionization (70 eV). Ions formed are guided to the time-of-flight chamber. A multi-channel plate (MCP) is used as a detector. The time resolution of AMS measurements was five seconds. One-minute detection limits for submicrometer particles are $< 0.04 \mu\text{g m}^{-3}$ for all species in the V-mode. The IGOR 6.11 (Wave-metrics, Lake Oswego, OR), Squirrel 1.53 (Sueper, 2013) and PIKA 1.12F were used to analyze the SP-AMS data.

Equipment used in the measurement of the CO, HC, and NO_x emissions conforms to the specifications of the Directive 70/220/EEC and its amendments. The true oxygen contents and densities of the fuels were used in the calculation of the results. A flame ionization detector (FID) was used for the measurement of hydrocarbons (all carbon-containing compounds, also oxygenates) (Sandström-Dahl et al., 2010; Aakko-Saksa et al., 2014). The calculation method chosen uses the density of 0.619 g dm^{-3} (different from the EC regulation 692/2008). A number of gaseous compounds (19 in total), amongst others nitrogen dioxide (NO₂), ammonia (NH₃), nitrous oxide (N₂O),

ethanol, formaldehyde and acetaldehyde were measured on-line with two-second time resolution using Fourier transformation infrared (FTIR) equipment (Gasmeter Cr-2000).

3 Results and discussion

3.1 Primary particulate and gaseous emissions of a gasoline passenger car

3.1.1 Particle size distributions

The driving cycle used in the study was NEDC being a statutory cycle in emission testing in Europe. The cycle consists of several patterns describing typical driving in urban environments and high-way driving (Fig. 1a) with total duration and length of the cycle is 1200 s and 11.0 km, respectively. Figure 1 shows the speed of the test vehicle during the test cycle and particle number concentration, particle volume concentration and particle size distribution of vehicle exhaust, all measured with high time resolution (1 s).

The exhaust particle number concentration was strongly dependent on driving condition (Fig. 1b). Large particle number concentrations were observed during accelerations, especially during the first two accelerations when the engine had not yet reached steady temperature conditions, and they were therefore associated with high engine loading and altering combustion conditions. In addition to soot particles (particle diameters of 30–100 nm, see Fig. 1c), there were also frequent observations of small particles ($D_p < 10$ nm), especially in the middle part of the cycle. These nanoparticles are most likely associated with deceleration and engine braking conditions (Rönkkö et al., 2014; Karjalainen et al., 2014). The largest particle volume concentrations were observed at the beginning, just after ignition and, on the other hand, at the end of the test cycle when the driving was at high speed and engine load. High total particle volume concentrations were strongly linked with the existence of soot mode particles in the exhaust.

Time-resolved primary and secondary particle emissions of a gasoline vehicle

P. Karjalainen et al.

Title Page

Abstract

Introduction

Conclusions

References

Tables

Figures

◀

▶

◀

▶

Back

Close

Full Screen / Esc

Printer-friendly Version

Interactive Discussion



3.1.2 Chemical composition

Figure 2 shows the chemical composition of primary exhaust particles during the NEDC cycle. The lower pane shows the major components, revealing that the large particle emission at the beginning of the cycle consists mainly of organic compounds and refractory black carbon (rBC). When compared to Fig. 1, it can be seen that the organic compounds together with rBC forms the so called soot mode, which dominate the particle volume concentration due to its large particle size. While the rBC has formed in the engine due to the incomplete combustion of fuel forming agglomerated soot particles (Heywood, 1988), the organic compounds have likely been condensed onto the soot particle surface mainly during cooling dilution process of exhaust. Figure 2 shows that later, after the starting phase of the test cycle the relative concentration of rBC decreases and remains at low levels with the exception of the accelerations at the highway part of the cycle. Interestingly, the concentration of organic compounds was very significant in the middle part of the cycle, i.e. when the emissions of nanoparticles (see Fig. 1) were observed to be high. Thus, while the high emission of organic compounds seems to be linked with high soot/rBC emission at the beginning of the cycle, in the middle part the organics and rBC emissions seemed not to be interlinked.

Concentrations of inorganic species (SO_4 , NH_4 , NO_3 , Cl) are shown in the upper pane of Fig. 2. Note that the concentration axes differ. In general, the highest sulfate and nitrate concentrations existed during accelerations, and had a good correlation with soot/rBC emissions. The sulfate concentration increases also during certain periods in the middle part of the cycle, clearly linked with similar peaks in organic compounds concentration (see Fig. 2). Interestingly, during highway driving and the following deceleration, also significant concentration of ammonium, nitrate and chloride ions were observed.

Time-resolved primary and secondary particle emissions of a gasoline vehicle

P. Karjalainen et al.

Title Page

Abstract

Introduction

Conclusions

References

Tables

Figures



Back

Close

Full Screen / Esc

Printer-friendly Version

Interactive Discussion

3.1.3 Gaseous emissions

The time series of total hydrocarbons, ammonia and NO_x during the NEDC test cycle are presented in Fig. 3. The largest hydrocarbon emissions were observed at the beginning of the cycle due to low engine and exhaust gas temperatures, which lowers the efficiency of the oxidation process in the three-way catalytic converter, in addition to higher formation rates of gaseous hydrocarbons during combustion. The hydrocarbon emissions are in line with the measurements of the chemical composition of particles, which shows that the highest emissions of particulate organic compounds occur at the beginning of the cycle. However, during the middle part of the cycle the emissions of gaseous hydrocarbons and organic particulate matter did not correlate; although in particle phase organics (see Fig. 2) the concentrations reached high values also during middle part of the cycle, the gaseous hydrocarbons remained at very low level until to the highway driving part of the cycle. The NO_x emissions were the highest at the beginning of the cycle and during the last part of the cycle when the driving speed and combustion temperatures were high. Ammonium concentrations were at the level of 10 ppm during most of the cycle, even higher than 100 ppm concentration was measured during the accelerations at the end of the cycle. The highest ammonia concentrations were clearly linked with acceleration, under conditions when the air-to-fuel ratio can be below 1 (rich mixture). This is in line with the findings by Meija-Centeno et al. (2007) and Heeb et al. (2006) showing ammonia formation in the three-way catalyst in slightly rich air-to-fuel ratios, which are prevailing during acceleration

3.2 Secondary particle emissions of a gasoline passenger car

3.2.1 Particle size distributions

Figure 4 shows the secondary particle number concentrations, volume concentrations and size distributions of gasoline passenger car exhaust during the NEDC cycle. In general, the volume and number concentrations as well as mean particle size of sec-

Time-resolved primary and secondary particle emissions of a gasoline vehicle

P. Karjalainen et al.

Title Page

Abstract

Introduction

Conclusions

References

Tables

Figures



Back

Close

Full Screen / Esc

Printer-friendly Version

Interactive Discussion



ondary particles were significantly larger than those of the primary particles, throughout the cycle. Periodic behaviour similar to that of the primary particles can be observed: first a period with large soot mode particles, then a period with a large number of small nanoparticles, and finally the highway part of the cycle.

As shown above, after the ignition the emissions of gaseous precursors (hydrocarbons and nitrogen containing species) and primary particles were observed to be high (Fig. 3). This combined with the information seen in Fig. 4 indicates that the existence of gaseous precursors in the exhaust significantly increases the secondary particulate matter formation, resulting as a high volume concentration of large particles at the beginning of the test cycle (Fig. 3). Compared to other periods of the cycle, at the beginning the volume concentration of secondary particles was three times higher, highlighting the role of cold starts in total secondary particle emission of gasoline vehicles.

The high oxidant concentrations in the PAM chamber result also in high concentrations of condensing compounds, which causes a possibility for nucleation in the chamber. In this study we measured higher particle number concentrations for the sample treated by the PAM than for the untreated sample. However, the increase of particle number was not very significant and, in principle, may also be caused by the increase of particle size into the measurement range of aerosol instruments. Interestingly, nanoparticles were not observed in the primary emission during the first period of cycle (Fig. 1), when both the precursor gas concentration and resulted volume of secondary particulate matter was the highest. During the first period, also the mean particle number concentrations were on a relatively similar level both in the primary and secondary aerosol. Instead, nanoparticles were observed in the sample treated by the PAM during the second phase (starting at 400 s) of the cycle. During this part of the test cycle the nanoparticles existed also in primary emissions. Thus the results indicate that nanoparticles found after PAM chamber are obviously initially formed already before the sample was introduced into the PAM chamber. It should be kept in mind that the existence and growth of nanoparticles in the PAM chamber can slightly change the

Time-resolved primary and secondary particle emissions of a gasoline vehicle

P. Karjalainen et al.

Title Page

Abstract

Introduction

Conclusions

References

Tables

Figures

◀

▶

◀

▶

Back

Close

Full Screen / Esc

Printer-friendly Version

Interactive Discussion



Time-resolved primary and secondary particle emissions of a gasoline vehicle

P. Karjalainen et al.

mean particle size and thus how effectively they are detected by aerosol instruments; e.g. the particle size range of aerosol mass spectrometers do not typically cover particles smaller than 50 nm, and in several studies the particle number size distribution measurement is limited to sizes above 10 nm.

As stated above, in the middle part of the cycle, a large number of primary nanoparticles was introduced into the chamber from the exhaust. Figure 3 shows that these sub-5 nm particles grew in the chamber to particle sizes similar to primary soot particles. This takes approximately 60–80 s, corresponding to the mean residence time in the PAM. In general, it seems that both the primary soot particles and primary nanoparticles can have an important role in secondary particle formation dynamics resulting e.g. in the size distribution of aged exhaust aerosol.

3.2.2 Chemical composition of secondary particles

The secondary aerosol mass consisted mainly of organic compounds and rBC (Fig. 5, lower pane). At the beginning of the test cycle, the concentrations of organic compounds in the secondary particulate matter were about 100 times higher than their concentrations in primary particles. During other parts of the cycle the concentrations of the organic compounds were significantly lower and remained relatively stable. The rBC concentration level did not change significantly because rBC is a primary component.

At the beginning of the cycle the incomplete combustion causes high emissions of rBC and gaseous hydrocarbons. Simultaneously the temperature of the three-way catalytic converter is low and thus the reduction of hydrocarbons is not optimal. In the PAM reactor, the oxidation of hydrocarbons lowers their volatility which results in high emissions of secondary particulate matter consisting of organic compounds. During highway part of the cycle, the incomplete combustion again causes the emission of soot/rBC during certain acceleration phases. However, during highway part the temperature of the catalyst used in the vehicle is very high, approximately 700 °C (see Karjalainen et al., 2014), meaning that it keeps the emissions of gaseous hydrocarbon

[Title Page](#)[Abstract](#)[Introduction](#)[Conclusions](#)[References](#)[Tables](#)[Figures](#)[◀](#)[▶](#)[◀](#)[▶](#)[Back](#)[Close](#)[Full Screen / Esc](#)[Printer-friendly Version](#)[Interactive Discussion](#)

emissions at a very low level. Thus, during the highway part the concentration of organic precursors is low in the exhaust, resulting in a low concentration of secondary organic particulate material.

In addition to rBC and organic compounds, during the middle part of the cycle the concentrations of inorganic species were observed to be stable. Only a slight increase in sulfate concentration was observed, simultaneously with the existence of nanoparticles in secondary aerosol. This observation is in line with primary particle measurements where sulfate peaks were observed during the middle part of the cycle. During the highway part of the cycle the concentrations of inorganic species in the secondary particulate matter increases when compared to the previous parts of the cycle. This is seemingly caused by high exhaust temperatures linked with high emissions of gaseous nitrogen compounds (see Fig. 3). Results indicate that also these compounds may have a significant role in traffic related secondary aerosol formation. However, this kind of aerosol is very specifically formed only at high vehicle speeds.

3.2.3 Influence of driving conditions to emission characteristics

The results presented above indicate that both the primary and secondary emissions vary strongly as a function of the driving cycle. To clarify the effects of driving conditions on the concentrations of secondary and primary particles the cycle was divided into three sections according to the engine and speed profile conditions: CSUDC (0–391 s), HUDC (392–787 s) and EUDC (788–1180 s). The CSUDC represents cold start situation, the HUDC represents typical city driving with warm engine and the EUDC represents typical highway driving. Figure 6 shows chemical composition and O : C ratios of primary and secondary exhaust particles for these three sections. O : C ratios were determined for organic compounds based on chemical composition measured by the SP-AMS, so that inorganic species and rBC were excluded. Emission factors for measured compounds are presented in the Supplement (see Fig. S1 and Table S1).

Primary particle emissions were dominated by rBC and organics. It should be noted that although the CSUDC and HUDC were similar from the viewpoint of driving condi-

Time-resolved primary and secondary particle emissions of a gasoline vehicle

P. Karjalainen et al.

Title Page

Abstract

Introduction

Conclusions

References

Tables

Figures

◀

▶

◀

▶

Back

Close

Full Screen / Esc

Printer-friendly Version

Interactive Discussion



tions, the rBC concentration was four times higher during CSUDC. Again, during the EUDC section of the cycle higher rBC concentration was observed in the exhaust. In contrast, for the organics similar differences between the sections of the test cycle were not observed. Inorganic species concentrations were relatively low in all cycle sections representing on average 3.6 % of particulate mass.

On average, the secondary particulate emissions were 13 times higher than the primary particle emissions. This value is higher or at similar level than observed in previous studies reported. For instance, Suarez-Bertoa et al. (2015) reported 2–4 times higher values for the secondary particle emissions of gasoline vehicle when compared to the primary organics and BC. In the diesel exhaust study of Chirico et al. (2010), the secondary and primary particle emissions were at similar level. However, in the study of Platt et al. (2013) SOA emission was around 14 times higher than primary organic aerosol (POA) emission when they measured the emissions of gasoline vehicle for the NEDC cycle. All of these studies were conducted using a batch chamber while in our study a flow through chamber was used. The differences between the studies can be due to the differences in the emissions but also due to the differences in wall losses.

The chemical composition of secondary particles differed significantly from primary particles; in secondary particles most of the particulate matter consisted of organics whereas the relative role of rBC was higher in primary particles. The calculative secondary organics concentration was high especially during CSUDC, even 9.9 mg m^{-3} . This highlights the important role primary and secondary emissions during cold start and the effects of emissions during cold start on atmospheric particulate pollutant levels. It should be noted that the emission factors of both primary and secondary particles were lowest during the EUDC (see Supplement).

O : C ratios were relatively stable for primary emissions, slightly higher O : C ratio (0.27) was observed for the CSUDC. Similar O : C ratios have been typically observed for fresh traffic emissions in urban ambient measurements (Timonen et al., 2013; Carbone et al., 2014). For the secondary emissions the O : C ratios were between 0.5–0.6. Large hydrocarbon emissions and probably differences in oxidation levels of primary

Time-resolved primary and secondary particle emissions of a gasoline vehicle

P. Karjalainen et al.

Title Page

Abstract

Introduction

Conclusions

References

Tables

Figures

◀

▶

◀

▶

Back

Close

Full Screen / Esc

Printer-friendly Version

Interactive Discussion



Time-resolved primary and secondary particle emissions of a gasoline vehicle

P. Karjalainen et al.

Title Page

Abstract

Introduction

Conclusions

References

Tables

Figures

◀

▶

◀

▶

Back

Close

Full Screen / Esc

Printer-friendly Version

Interactive Discussion

with a warmed engine produced significantly lower primary and secondary particulate emissions. This indicates that the adverse effects of traffic are likely to be the largest in city areas where driving distances are typically short, near houses and workplaces. However, we note that the formation of secondary particulate matter is a longer-time atmospheric process and thus not directly linked with human exposure and human health at the site of emission. Also, it is reasonable to assume that this problem at least from the viewpoint of secondary aerosol precursor emissions is magnified under cold climatic conditions.

Both primary and secondary emissions were highly dependent on driving conditions, such as speed, acceleration and deceleration profiles. At high speed (EUDC), both particulate mass and size distribution were different when compared to low speed driving (HUCD). In addition, under deceleration conditions very small nanoparticles were observed in primary exhaust. These nanoparticles grew in particle size due to the condensation of highly oxidized engine origin compounds; these oxidized compounds were formed in our experiment in the PAM chamber but in reality they are formed in the atmosphere. Thus, our results indicate that also nanoparticles can contribute to atmospheric secondary aerosol formation, especially on size distribution of secondary particles. Due to that it is clear that current legislation focusing on larger particles (PM mass or number of particles larger than 23 nm in diameter) is not optimal from the viewpoint of realistic urban air quality, since it takes into account only the largest primary particles.

This study highlights the importance of reduction of precursor gases as mean to reduce secondary pollutants. A reduction of the emission of precursor gases can be achieved by properly designed emission control technologies. Also by smart city planning it is possible to reduce PM emissions by reducing the driving conditions where PM and precursor gas emissions are large e.g. acceleration/deceleration needs or congestion. These topics should be taken into account in the future legislation, especially because currently vehicles are generally low primary PM emitters, while the emissions of secondary aerosol precursors can still remain high. In order to protect citizens from the

Time-resolved primary and secondary particle emissions of a gasoline vehicle

P. Karjalainen et al.

Title Page

Abstract

Introduction

Conclusions

References

Tables

Figures

◀

▶

◀

▶

Back

Close

Full Screen / Esc

Printer-friendly Version

Interactive Discussion



- Braisher, M., Stone, R., and Price, P.: Particle Number Emissions from a Range of European Vehicles, SAE Technical Paper, 2010-01-0786, doi:10.4271/2010-01-0786, 2010.
- CARB: Proposed amendments to Californias low-emission vehicle regulations – particulate matter mass, ultrafine solid particle number, and black carbon emissions, Workshop report, California Air Resources Board, 18 May 2010, El Monte, California, 1–24, 2010.
- Carbone, S., Aurela, M., Saarnio, K., Saarikoski, S., Timonen, H., Frey, A., Sueper, D., Ulbrich, I. M., Jimenez, J. L., Kulmala, M., Worsnop, D. R., and Hillamo, R. E.: Wintertime aerosol chemistry in sub-Arctic urban air, *Aerosol Sci. Tech.*, 48, 313–323, doi:10.1080/02786826.2013.875115, 2014.
- Chase, R. E., Duszkiwicz, G. J., Richert, J. F. O., Lewis, D., Maricq, M. M., and Xu, N.: PM Measurement Artifact: Organic Vapor Deposition on Different Filter Media, SAE Technical Paper, 2004-01-0967, doi:10.4271/2004-01-0967, 2004.
- Chirico, R., DeCarlo, P. F., Heringa, M. F., Tritscher, T., Richter, R., Prévôt, A. S. H., Dommen, J., Weingartner, E., Wehrle, G., Gysel, M., Laborde, M., and Baltensperger, U.: Impact of aftertreatment devices on primary emissions and secondary organic aerosol formation potential from in-use diesel vehicles: results from smog chamber experiments, *Atmos. Chem. Phys.*, 10, 11545–11563, doi:10.5194/acp-10-11545-2010, 2010.
- DeCarlo, P. F., Kimmel, J. R., Trimborn, A., Northway, M. J., Jayne, J. T., Aiken, A. C., Gonin, M., Fuhrer, K., Horvath, T., Docherty, K. S., Worsnop, D. R., and Jimenez, J. L.: Field-deployable, high-resolution, time-of-flight aerosol mass spectrometer, *Anal. Chem.*, 78, 8281–8289, doi:10.1021/ac061249n, 2006.
- Gordon, T. D., Tkacik, D. S., Presto, A. A., Zhang, M., Jathar, S. H., Nguyen, N. T., Massetti, J., Truong, T., Cicero-Fernandez, P., Maddox, C., Rieger, P., Chattopadhyay, S., Maldonado, H., Maricq, M. M., and Robinson, A. L.: Primary gas- and particle-phase emissions and secondary organic aerosol production from gasoline and diesel off-road engines, *Environ. Sci. Technol.*, 47, 14137–14146, doi:10.1021/es403556e, 2013.
- Harris, S. J. and Maricq, M. M.: Signature size distributions for diesel and gasoline engine exhaust particulate matter, *J. Aerosol Sci.*, 32, 749–764, doi:10.1016/S0021-8502(00)00111-7, 2001.
- Heeb, N. V., Forss, J. A.-M., Brühlmann, S., Lüscher, R., Saxer, C. J., and Hug, P.: Correlation of hydrogen, ammonia and nitrogen monoxide (nitric oxide) emissions of gasoline-fueled Euro-3 passenger cars at transient driving, *Atmos. Environ.*, 40, 3750–3763, doi:10.1016/j.atmosenv.2006.03.002, 2006.

Time-resolved primary and secondary particle emissions of a gasoline vehicle

P. Karjalainen et al.

- Heywood, J. B.: *Internal Combustion Engine Fundamentals*, McGraw-Hill Education, New York, 1988.
- Högström, R., Karjalainen, P., Yli-Ojanperä, J., Rostedt, A., Heinonen, M., Mäkelä, J. M., and Keskinen, J.: Study of the PM gas-phase filter artifact using a setup for mixing diesel-like soot and hydrocarbons, *Aerosol Sci. Tech.*, 46, 1045–1052, doi:10.1080/02786826.2012.689118, 2012.
- Jayne, J. T., Leard, D. C., Zhang, X., Davidovits, P., Smith, K. A., Kolb, C. E., and Worsnop, D. R.: Development of an aerosol mass spectrometer for size and composition analysis of submicron particles, *Aerosol Sci. Tech.*, 33, 49–70, doi:10.1080/027868200410840, 2000.
- Johnson, T., Caldow, R., Pocher, A., Mirmem, A., and Kittelson, D.: A New Electrical Mobility Particle Sizer Spectrometer for Engine Exhaust Particle Measurements, *SAE Technical Paper*, 2004-01-13, doi:10.4271/2004-01-1341, 2004.
- Kang, E., Root, M. J., Toohey, D. W., and Brune, W. H.: Introducing the concept of Potential Aerosol Mass (PAM), *Atmos. Chem. Phys.*, 7, 5727–5744, doi:10.5194/acp-7-5727-2007, 2007.
- Kang, E., Toohey, D. W., and Brune, W. H.: Dependence of SOA oxidation on organic aerosol mass concentration and OH exposure: experimental PAM chamber studies, *Atmos. Chem. Phys.*, 11, 1837–1852, doi:10.5194/acp-11-1837-2011, 2011.
- Karjalainen, P., Pirjola, L., Heikkilä, J., Lähde, T., Tzamkiozis, T., Ntziachristos, L., Keskinen, J., and Rönkkö, T.: Exhaust particles of modern gasoline vehicles: a laboratory and an on-road study, *Atmos. Environ.*, 97, 262–270, doi:10.1016/j.atmosenv.2014.08.025, 2014.
- Keskinen, J. and Rönkkö, T.: Can real-world diesel exhaust particle size distribution be reproduced in the laboratory? A critical review, *J. Air Waste Manage.*, 60, 1245–1255, doi:10.3155/1047-3289.60.10.1245, 2010.
- Khalek, I. A., Bougher, T., and Jetter, J. J.: Particle emissions from a 2009 gasoline direct injection engine using different commercially available fuels, *SAE Int. J. Fuels Lubr.*, 3, 623–637, doi:10.4271/2010-01-2117, 2010.
- Lahde, T., Niemi, J. V, Kousa, A., Ronkko, T., Karjalainen, P., Keskinen, J., Frey, A., Hillamo, R., and Pirjola, L.: Mobile particle and NO_x emission characterization at Helsinki Downtown: comparison of different traffic flow areas, *Aerosol Air Qual. Res.*, 14, 1372–1382, doi:10.4209/aaqr.2013.10.0311, 2014.
- Lambe, A. T., Ahern, A. T., Williams, L. R., Slowik, J. G., Wong, J. P. S., Abbatt, J. P. D., Brune, W. H., Ng, N. L., Wright, J. P., Croasdale, D. R., Worsnop, D. R., Davidovits, P.,

Title Page

Abstract

Introduction

Conclusions

References

Tables

Figures

◀

▶

◀

▶

Back

Close

Full Screen / Esc

Printer-friendly Version

Interactive Discussion

**Time-resolved
primary and
secondary particle
emissions of a
gasoline vehicle**

P. Karjalainen et al.

Title Page

Abstract

Introduction

Conclusions

References

Tables

Figures

◀

▶

◀

▶

Back

Close

Full Screen / Esc

Printer-friendly Version

Interactive Discussion



and Onasch, T. B.: Characterization of aerosol photooxidation flow reactors: heterogeneous oxidation, secondary organic aerosol formation and cloud condensation nuclei activity measurements, *Atmos. Meas. Tech.*, 4, 445–461, doi:10.5194/amt-4-445-2011, 2011.

Li, T., Chen, X., and Yan, Z.: Comparison of fine particles emissions of light-duty gasoline vehicles from chassis dynamometer tests and on-road measurements, *Atmos. Environ.*, 68, 82–91, doi:10.1016/j.atmosenv.2012.11.031, 2013.

Maricq, M., Podsiadlik, D., Brehob, D., and Haghgooe, M.: Particulate emissions from a direct-injection spark-ignition (DISI) engine, SAE Technical Paper, 1999-01-1530, doi:10.4271/1999-01-1530, 1999.

Maricq, M. M., Szente, J. J., and Jahr, K.: The impact of ethanol fuel blends on PM emissions from a light-duty GDI vehicle, *Aerosol Sci. Tech.*, 46, 576–583, doi:10.1080/02786826.2011.648780, 2012.

Mathis, U., Mohr, M., and Forss, A.: Comprehensive particle characterization of modern gasoline and diesel passenger cars at low ambient temperatures, *Atmos. Environ.*, 39, 107–117, doi:10.1016/j.atmosenv.2004.09.029, 2005.

Mejia-Centeno, I., Martínez-Hernández, A., and Fuentes, G.: Effect of low-sulfur fuels upon NH_3 and N_2O emission during operation of commercial three-way catalytic converters, *Top. Catal.*, 42–43, 381–385, doi:10.1007/s11244-007-0210-2, 2007.

Mohr, M., Forss, A., and Lehmann, U.: Particle emissions from diesel passenger cars equipped with a particle trap in comparison to other technologies, *Environ. Sci. Technol.*, 40, 2375–2383, doi:10.1021/es051440z, 2006.

Nordin, E. Z., Eriksson, A. C., Roldin, P., Nilsson, P. T., Carlsson, J. E., Kajos, M. K., Helén, H., Wittbom, C., Rissler, J., Löndahl, J., Swietlicki, E., Svenningsson, B., Bohgard, M., Kulmala, M., Hallquist, M., and Pagels, J. H.: Secondary organic aerosol formation from idling gasoline passenger vehicle emissions investigated in a smog chamber, *Atmos. Chem. Phys.*, 13, 6101–6116, doi:10.5194/acp-13-6101-2013, 2013.

Ntziachristos, L., Giechaskiel, B., Pistikopoulos, P., Samaras, Z., Mathis, U., Mohr, M., Ristimäki, J., Keskinen, J., Mikkanen, P., Casati, R., Scheer, V., and Vogt, R.: Performance evaluation of a novel sampling and measurement system for exhaust particle characterization, SAE Technical Paper, 2004-01-1439, doi:10.4271/2004-01-1439, 2004.

Ortega, A. M., Day, D. A., Cubison, M. J., Brune, W. H., Bon, D., de Gouw, J. A., and Jimenez, J. L.: Secondary organic aerosol formation and primary organic aerosol oxida-

**Time-resolved
primary and
secondary particle
emissions of a
gasoline vehicle**

P. Karjalainen et al.

Title Page

Abstract

Introduction

Conclusions

References

Tables

Figures

◀

▶

◀

▶

Back

Close

Full Screen / Esc

Printer-friendly Version

Interactive Discussion

tion from biomass-burning smoke in a flow reactor during FLAME-3, *Atmos. Chem. Phys.*, 13, 11551–11571, doi:10.5194/acp-13-11551-2013, 2013.

Pierce, J. R., Engelhart, G. J., Hildebrandt, L., Weitkamp, E. A., Pathak, R. K., Donahue, N. M., Robinson, A. L., Adams, P. J., and Pandis, S. N.: Constraining particle evolution from wall losses, coagulation, and condensation-evaporation in smog-chamber experiments: optimal estimation based on size distribution measurements, *Aerosol Sci. Tech.*, 42, 1001–1015, doi:10.1080/02786820802389251, 2008.

Pirjola, L., Lähde, T., Niemi, J. V., Kousa, A., Rönkkö, T., Karjalainen, P., Keskinen, J., Frey, A., and Hillamo, R.: Spatial and temporal characterization of traffic emissions in urban microenvironments with a mobile laboratory, *Atmos. Environ.*, 63, 156–167, doi:10.1016/j.atmosenv.2012.09.022, 2012.

Pirjola, L., Karjalainen, P., Heikkilä, J., Saari, S., Tzamkiozis, T., Ntziachristos, L., Kulmala, K., Keskinen, J., and Rönkkö, T.: Effects of fresh lubricant oils on particle emissions emitted by a modern gasoline direct injection passenger car, *Environ. Sci. Technol.*, 49, 3644–3652, doi:10.1021/es505109u, 2015a.

Pirjola, L., Karl, M., Rönkkö, T., and Arnold, F.: Model studies of volatile diesel exhaust particle formation: organic vapours involved in nucleation and growth?, *Atmos. Chem. Phys. Discuss.*, 15, 4219–4263, doi:10.5194/acpd-15-4219-2015, 2015b.

Platt, S. M., El Haddad, I., Zardini, A. A., Clairotte, M., Astorga, C., Wolf, R., Slowik, J. G., Temime-Roussel, B., Marchand, N., Ježek, I., Drinovec, L., Močnik, G., Möhler, O., Richter, R., Barmet, P., Bianchi, F., Baltensperger, U., and Prévôt, A. S. H.: Secondary organic aerosol formation from gasoline vehicle emissions in a new mobile environmental reaction chamber, *Atmos. Chem. Phys.*, 13, 9141–9158, doi:10.5194/acp-13-9141-2013, 2013.

Pope III, C. A. and Dockery, D. W.: 2006 critical review: health effects of fine particulate air pollution: lines that connect, *J. Air Waste Manage.*, 56, 709–742, 2006.

Pourkhesalian, A. M., Stevanovic, S., Rahman, M. M., Faghihi, E. M., Bottle, S. E., Masri, A. R., Brown, R. J., and Ristovski, Z. D.: Effect of atmospheric aging on volatility and reactive oxygen species of biodiesel exhaust nano-particles, *Atmos. Chem. Phys.*, 15, 9099–9108, doi:10.5194/acp-15-9099-2015, 2015.

Robinson, A. L., Donahue, N. M., Shrivastava, M. K., Weitkamp, E. A., Sage, A. M., Grieshop, A. P., Lane, T. E., Pierce, J. R., and Pandis, S. N.: Rethinking organic aerosols: semivolatile emissions and photochemical aging, *Science*, 315, 1259–1262, doi:10.1126/science.1133061, 2007.

Time-resolved primary and secondary particle emissions of a gasoline vehicle

P. Karjalainen et al.

Title Page

Abstract

Introduction

Conclusions

References

Tables

Figures

◀

▶

◀

▶

Back

Close

Full Screen / Esc

Printer-friendly Version

Interactive Discussion

- Rogge, W. F., Hildemann, L. M., Mazurek, M. a., Cass, G. R., and Simoneit, B. R. T.: Sources of fine organic aerosol. 2. Noncatalyst and catalyst-equipped automobiles and heavy-duty diesel trucks, *Environ. Sci. Technol.*, 27, 636–651, doi:10.1021/es00041a007, 1993.
- 5 Rönkkö, T., Virtanen, A., Vaaraslahti, K., Keskinen, J., Pirjola, L., and Lappi, M.: Effect of dilution conditions and driving parameters on nucleation mode particles in diesel exhaust: laboratory and on-road study, *Atmos. Environ.*, 40, 2893–2901, doi:10.1016/j.atmosenv.2006.01.002, 2006.
- Rönkkö, T., Pirjola, L., Ntziachristos, L., Heikkilä, J., Karjalainen, P., Hillamo, R., and Keskinen, J.: Vehicle engines produce exhaust nanoparticles even when not fueled, *Environ. Sci. Technol.*, 48, 2043–2050, doi:10.1021/es405687m, 2014.
- 10 Sakurai, H., Tobias, H. J., Park, K., Zarling, D., Docherty, K. S., Kittelson, D. B., McMurry, P. H., and Ziemann, P. J.: On-line measurements of diesel nanoparticle composition and volatility, *Atmos. Environ.*, 37, 1199–1210, doi:10.1016/S1352-2310(02)01017-8, 2003.
- Sandström-Dahl, C., Erlandsson, L., Gasste, J., and Lindgren, M.: Measurement methodologies for hydrocarbons, ethanol and aldehyde emissions from ethanol fuelled vehicles, *SAE Int. J. Fuels Lubr.*, 3, 453–466, doi:10.4271/2010-01-1557, 2010.
- 15 Schwarz, J. P., Spackman, J. R., Fahey, D. W., Gao, R. S., Lohmann, U., Stier, P., Watts, L. A., Thomson, D. S., Lack, D. a., Pfister, L., Mahoney, M. J., Baumgardner, D., Wilson, J. C., and Reeves, J. M.: Coatings and their enhancement of black carbon light absorption in the tropical atmosphere, *J. Geophys. Res.-Atmos.*, 113, 1–10, doi:10.1029/2007JD009042, 2008.
- Sementa, P., Maria Vaglieco, B., and Catapano, F.: Thermodynamic and optical characterizations of a high performance GDI engine operating in homogeneous and stratified charge mixture conditions fueled with gasoline and bio-ethanol, *Fuel*, 96, 204–219, doi:10.1016/j.fuel.2011.12.068, 2012.
- 25 Sgro, L. A., Sementa, P., Vaglieco, B. M., Rusciano, G., D’Anna, A., and Minutolo, P.: Investigating the origin of nuclei particles in GDI engine exhausts, *Combust. Flame*, 159, 1687–1692, doi:10.1016/j.combustflame.2011.12.013, 2012.
- Suarez-Bertoa, R., Zardini, A. A., Keuken, H., and Astorga, C.: Impact of ethanol containing gasoline blends on emissions from a flex-fuel vehicle tested over the Worldwide Harmonized Light duty Test Cycle (WLTC), *Fuel*, 143, 173–182, doi:10.1016/j.fuel.2014.10.076, 2015.
- 30 Timonen, H., Carbone, S., Aurela, M., Saarnio, K., Saarikoski, S., Ng, N. L., Canagaratna, M. R., Kulmala, M., Kerminen, V. M., Worsnop, D. R., and Hillamo, R.: Charac-

**Time-resolved
primary and
secondary particle
emissions of a
gasoline vehicle**

P. Karjalainen et al.

Title Page

Abstract

Introduction

Conclusions

References

Tables

Figures

◀

▶

◀

▶

Back

Close

Full Screen / Esc

Printer-friendly Version

Interactive Discussion

teristics, sources and water-solubility of ambient submicron organic aerosol in springtime in Helsinki, Finland, *J. Aerosol Sci.*, 56, 61–77, doi:10.1016/j.jaerosci.2012.06.005, 2013.

Tkacik, D. S., Lambe, A. T., Jathar, S., Li, X., Presto, A. A., Zhao, Y., Blake, D., Meinardi, S., Jayne, J. T., Croteau, P. L., and Robinson, A. L.: Secondary organic aerosol formation from in-use motor vehicle emissions using a potential aerosol mass reactor, *Environ. Sci. Technol.*, 48, 11235–11242, doi:10.1021/es502239v, 2014.

Tobias, H. J., Beving, D. E., Ziemann, P. J., Sakurai, H., Zuk, M., McMurry, P. H., Zarling, D., Waytulonis, R., and Kittelson, D. B.: Chemical analysis of diesel engine nanoparticles using a nano-DMA/thermal desorption particle beam mass spectrometer, *Environ. Sci. Technol.*, 35, 2233–2243, 2001.

Wehner, B., Birmili, W., Gnauk, T., and Wiedensohler, A.: Particle number size distributions in a street canyon and their transformation into the urban-air background: measurements and a simple model study, *Atmos. Environ.*, 36, 2215–2223, doi:10.1016/S1352-2310(02)00174-7, 2002.

Weitkamp, E. A., Sage, A. M., Pierce, J. R., Donahue, N. M., and Robinson, A. L.: Organic aerosol formation from photochemical oxidation of diesel exhaust, *Environ. Sci. Technol.*, 41, 6969–6975, 2007.

Time-resolved primary and secondary particle emissions of a gasoline vehicle

P. Karjalainen et al.

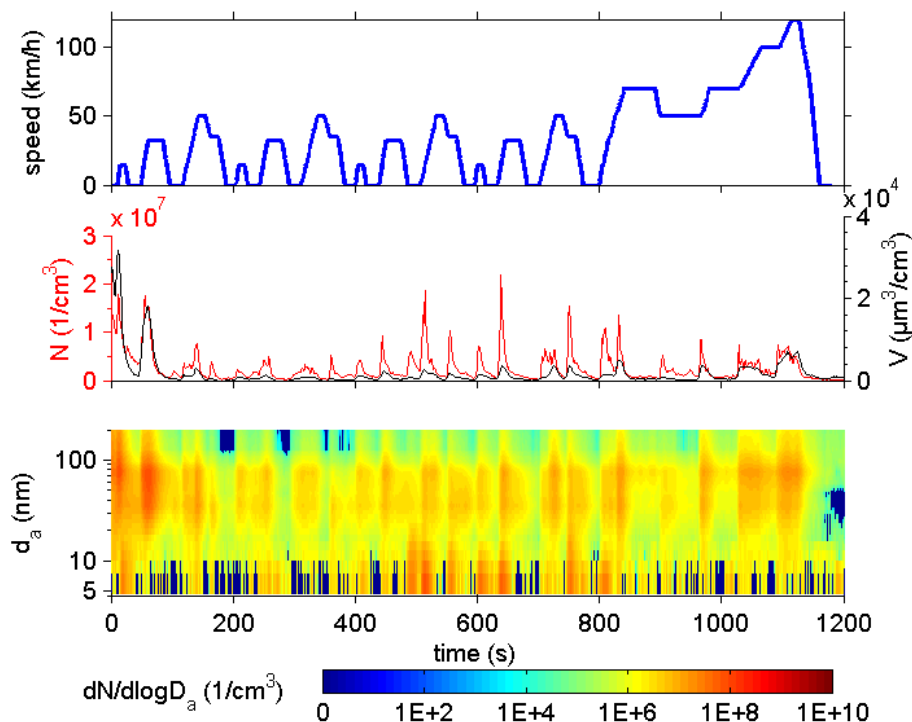


Figure 1. Speed profile, primary particle number (measured by the CPC) and volume concentrations (measured by HRLPI) and primary particle size distributions (HRLPI) for the studied gasoline passenger car during the NEDC test cycle.

Time-resolved primary and secondary particle emissions of a gasoline vehicle

P. Karjalainen et al.

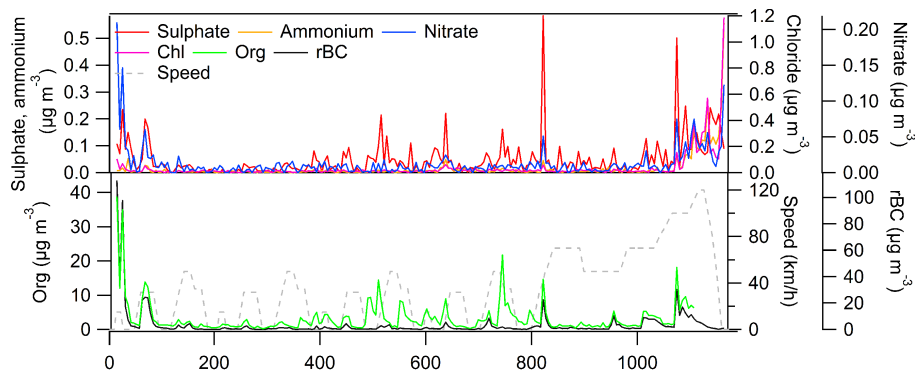


Figure 2. Temporal behavior of rBC, organics, SO_4 , NO_3 and NH_4 concentrations measured by the SP-AMS for the primary emissions (without the PAM chamber) during the NEDC test cycle.

Title Page

Abstract

Introduction

Conclusions

References

Tables

Figures

◀

▶

◀

▶

Back

Close

Full Screen / Esc

Printer-friendly Version

Interactive Discussion

Time-resolved primary and secondary particle emissions of a gasoline vehicle

P. Karjalainen et al.

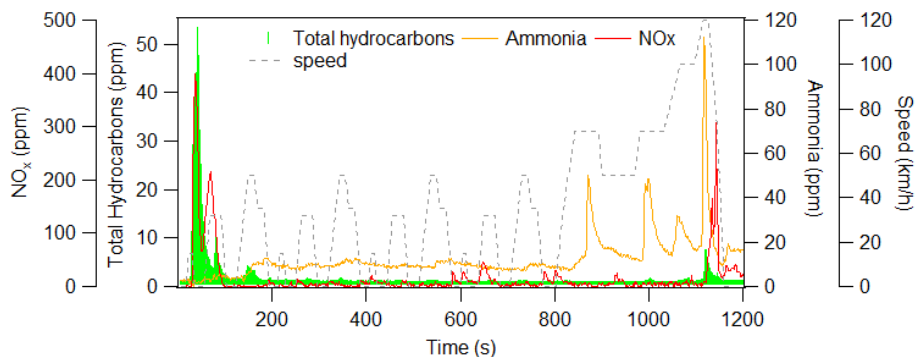


Figure 3. Time-series of the exhaust concentrations of total hydrocarbons, ammonia and NO_x.

Title Page

Abstract

Introduction

Conclusions

References

Tables

Figures

◀

▶

◀

▶

Back

Close

Full Screen / Esc

Printer-friendly Version

Interactive Discussion

Time-resolved primary and secondary particle emissions of a gasoline vehicle

P. Karjalainen et al.

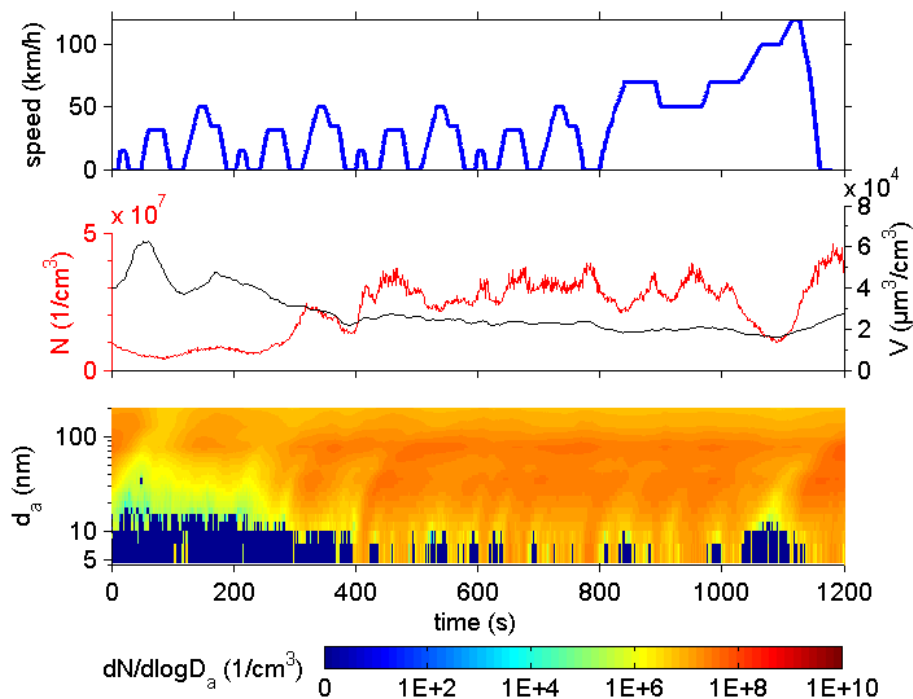


Figure 4. Speed profile, secondary particle number (measured by the CPC) and volume concentrations (measured by the HRLPI) and secondary particle number size distributions (HRLPI) for the studied gasoline passenger car during the NEDC test cycle.

Time-resolved primary and secondary particle emissions of a gasoline vehicle

P. Karjalainen et al.

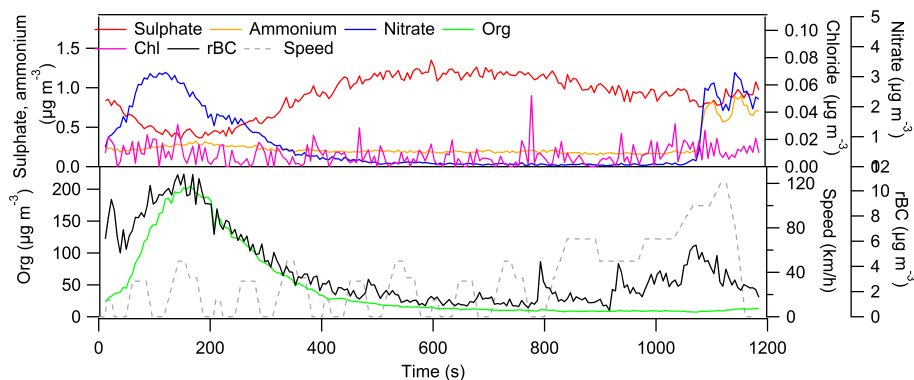


Figure 5. Temporal behavior of rBC, organics, SO_4 , NO_3 , NH_4 and Chl concentrations measured by the SP-AMS downstream of the PAM chamber during the NEDC test cycle.

[Title Page](#)[Abstract](#)[Introduction](#)[Conclusions](#)[References](#)[Tables](#)[Figures](#)[◀](#)[▶](#)[◀](#)[▶](#)[Back](#)[Close](#)[Full Screen / Esc](#)[Printer-friendly Version](#)[Interactive Discussion](#)

Time-resolved primary and secondary particle emissions of a gasoline vehicle

P. Karjalainen et al.

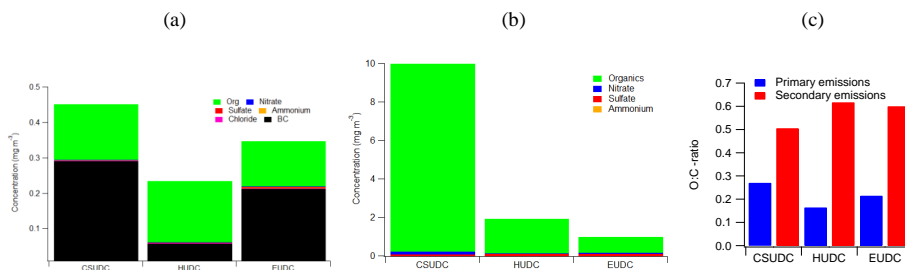


Figure 6. Chemical composition of primary (a) and secondary (b) particulate material and the O:C ratios of primary and secondary particulate matter (c) for different parts of the NEDC cycle.